PHYSICAL REVIEW E **100**, 012709 (2019)

Phase behavior of hard C_{2h}-symmetric particle systems

Christian D'Urso and Giorgio Celebre
Dipartimento di Chimica e Tecnologie Chimiche, Università della Calabria, via P. Bucci, I-87036 Arcavacata di Rende (CS), Italy

Giorgio Cinacchi[*]
Departamento de Física Teórica de la Materia Condensada, Instituto de Física de la Materia Condensada (IFIMAC),
Instituto de Ciencias de Materiales "Nicolás Cabrera," Universidad Autónoma de Madrid, Ciudad Universitaria de Cantoblanco,
E-28049 Madrid, Spain

(Received 16 April 2019; published 30 July 2019)

Using Monte Carlo numerical simulation, this work sketches the phase diagram of systems of certain hard C_{2h}-symmetric particles, formed by gluing two aligned and displaced hard spherocylinders with a cylindrical-length-to-diameter ratio realistically, if viewed not only from the lyotropic colloidal liquid-crystal side but also from the thermotropic low-molecular-mass liquid-crystal side, equal to 5, as a function of the displacement. Several distinctive phases are observed, such as a nonperiodic smectic-*B*-like phase, a nonperiodic smectic-*H*-like phase, a smectic-*C* phase, and a short-layer-spacing uniaxial smectic-*A* phase but no biaxial nematic phase.

DOI: 10.1103/PhysRevE.100.012709

I. INTRODUCTION

Within the broad (soft) condensed matter [1], liquid crystals (LCs) [2], with their combination of fluidity and (partial) order, occupy a special place. Of the several liquid-crystalline phases, the uniaxial nematic (N_u) phase is the simplest. In the bulk of this $D_{\infty h}$-symmetric fluid phase, the system constituent, sufficiently elongate (rodlike) or sufficiently flat (disklike) particles, while positionally uniformly distributed, preferentially orient their primary axis along a common (fixed) direction, the major director $\hat{n}$. More complex is the (orthorhombic) biaxial nematic (N_{bo}) phase. In the bulk of this D_{2h}-symmetric fluid phase, besides the particle positionally uniform distribution and the orientational ordering of the particle primary axis, the particle secondary axis also preferentially orients along one more common (fixed) direction, the minor director $\hat{m}$, such that $\hat{m} \perp \hat{n}$ and then $\hat{l} = \hat{m} \times \hat{n}$. The commonness of the N_u phase (naturally a quite mandatory condition, together with its special attributes, for its widespread use in technology) contrasts with the rarity of the N_{bo} phase, a continual focus of many theoretical and experimental investigations [3–41].

Though, in a ideal(istic) system, the N_{bo} phase can be artificially injected into the phase diagram or its thermodynamic stability artificially swollen [42], in a real(istic) system, even leaving aside the issue of its existence right under those (strict) ambient conditions of pressure and temperature that would make it really usable in technology, the *per se* formation of such a phase, truly fluid, spontaneous, and thermodynamically stable, appears very difficult. In fact, it requires the freezing of the additional orientational degree of freedom not be accompanied by any onset of partial positional ordering, be it layering (smectic phase formation) or stacking (columnar phase formation), or solidification, be it crystallization or vitrification.

It may not come as a surprise that the very few experimental systems in which the existence of this phase has been reasonably confirmed belong to the classes of lyotropic [7,30] and thermotropic polymeric [8,22] LCs. While their large size naturally allows achieving a large shape nonsphericity, thus favoring liquid crystallinity, their polydispersity further disfavors partial positional ordering and crystallization (not vitrification though: in fact, the observation of biaxial nematic ordering in thermotropic polymeric LCs appears rather linked to the occurrence of a glass transition [8,22]). In the class of thermotropic low-molecular-mass LCs [43], limited, compared to thermotropic polymeric LCs, by the small size, and further limited, compared to lyotropic LCs, by the atomic nature, the small number, and the chemistry of their building blocks (the typical chemical elements of organic chemistry) and, as molecular fluids, afflicted by miscibility problems, all the claims, made over the years, of having experimentally observed a biaxial nematic phase have thus far been unable to rise to the status of undisputed fact [44].

In an attempt to contribute to this persistently debated issue, this work investigates, via numerical simulation, the phase behavior of pure systems composed of certain continuously translating and rotating hard C_{2h}-symmetric particles to probe their propensity to exhibit a N_{bo} phase.

Next Sec. II describes these model particles and motives their choice; Sec. III describes the method chosen to investigate systems of them as well as provides the definition of most of the quantities that were calculated to characterize the phases that such systems form; Sec. IV and the Supplemental Material [45] present the obtained results while Sec. V draws from these results a few conclusions.

II. MODEL

The model particles that this work considers are dimers of hard congruent and parallel spherocylinders, i.e., cylinders of length L capped at both ends with hemispheres of the same

---

[*] giorgio.cinacchi@uam.es

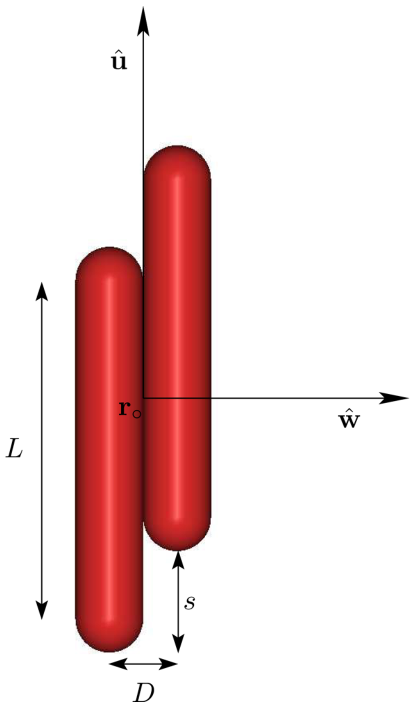

FIG. 1. Image of a hard spherocylinder dimer, with indicated: the geometrical parameters defining its shape and size: L, the length of the cylindrical part, D, the diameter, and s, the shift; the vectors defining its (configurational) mechanical state in the laboratory reference frame: $\mathbf{r}_\circ$, the position of the hard spherocylinder dimer centroid and $\{\hat{\mathbf{u}}, \hat{\mathbf{v}}, \hat{\mathbf{w}}\}$, the triad of unit vectors, with $\hat{\mathbf{v}} = \hat{\mathbf{u}} \times \hat{\mathbf{w}}$, specifying the hard spherocylinder dimer orientation.

diameter D [47], whose centroids are shifted by a distance s along the direction of their C_∞ axis $\hat{\mathbf{u}}$ and by a distance D along the direction of one of their C_2 axes $\hat{\mathbf{w}}$ (Fig. 1). There are several reasons for considering these model particles:

(1) The particles are C_{2h}-symmetric because it was hypothesized that this symmetry encompasses particle shapes that might not promote the formation of a well-defined smectic phase, thus possibly widening the stability range of the nematic phase at higher density, then giving biaxial nematic ordering more chance to turn up. The C_{2h} symmetry choice was not driven by a hope of observing a biaxial nematic phase other than [29,31,48] the already evanescent N_{bo} phase.

(2) The particles have been assumed to interact via hard interactions for two subreasons.

(a) In the spirit of Occam's razor [49], short-range steeply repulsive intermolecular interactions due to particle shape and size are most objectively quantifiable. Despite years of research work, both the accurate magnitude and orientation dependence of long-range attractive (dispersion) intermolecular interactions cannot truly reliably be predicted yet [50]. Therefore, model nonspherical particles that incorporate them and specify their magnitude and orientation dependence inevitably and uncomfortably suffer from a certain degree of arbitrariness.

(b) It is well known that short-range repulsive interparticle interactions are those mainly responsible for the thermodynamic, structural, and dynamic properties of many condensed matter systems [51,52]. This holds true not only for lyotropic colloidal LCs, suitably synthesized colloidal particles being good experimental realization of hard particles [53], but also for thermotropic molecular LCs, irrespective of the marginal role that the temperature T has in the behavior of a hard-particle system. Just recalling the role played by the hard-sphere model in explaining many aspects of the behavior of systems of monoatomic molecules and the parallelism that exists between a pure system of hard spheres and a pure system of particles interacting via the Lennard-Jones potential energy model [54,55] should dispel any critique of unreality that could be thrown on a hard nonspherical particle model anytime it is used to address problems relevant to thermotropic molecular LCs.

(3) The particles are made as dimers of hard spherocylinders because of the simplicity of the hard-spherocylinder overlap criterion [56] and their capability, as monomers, to form a smectic phase [57,58]. Hard prolate ellipsoids were deliberately avoided not just because of their more complicated overlap criterion [59,60] but especially because of the willingness not to bias a system of such hard dimers in its capability to form a positionally ordered phase by constructing them with hard prolate ellipsoid (or similarly shaped) monomers, known not to form any smectic phase [61–63].

(4) The dimers are identical to investigate a pure system and assess whether it alone is able to exhibit a biaxial nematic phase. While lyotropic and polymeric LCs are polydisperse and this feature is usually welcome in the effort to stabilizing a biaxial nematic phase by destabilizing the positionally ordered phases, thermotropic low-molecular-mass LCs cannot have that continuous variation of shapes and sizes while being potentially afflicted by miscibility problems [64].

(5) The dimers are made of hard spherocylinder monomers with a moderate aspect ratio $L/D = 5$ not just because systems of these specific hard spherocylinder monomers have been among those most investigated [58] but especially because such an aspect ratio is reasonably consistent with those typical of thermotropic low-molecular-mass nematogens and smectogens. Considering hard biaxial particles with large values of both the height-to-breadth ratio and breadth-to-width ratio clearly and unsurprisingly promotes, at sufficiently high density, the formation of a biaxial nematic phase inasmuch considering hard elongate uniaxial particles with a large length-to-width ratio promotes, at sufficiently high density, the formation of a uniaxial nematic phase: that irrespective of their actual shape [41,68]. Unfortunately, such large values of height-to-breadth ratio and breath-to-width ratio cannot be displayed by thermotropic low-molecular-mass LCs. The difficulty is rather to find one, if any, hard biaxial particle model of such a "chiseled" shape so as to promote the formation of a thermodynamically stable biaxial nematic phase while keeping its size moderate [69] as well as being susceptible of being rendered by chemical molecular synthesis [70].

(6) The dimers are continuously translating and rotating. On one hand, while certainly of utility in addressing aspects of the phase transitions involving a biaxial nematic phase, usual lattice models [14] do not clearly allow for the existence of positionally ordered phases. On the other hand, constraining the particle orientations to be discrete and few, e.g., perfectly

parallel [20] or at most aligning along the three axes of the laboratory reference frame [33] (Zwanzig model [71]), while certainly a very friendly approximation for any theoretical calculation, it is clearly unrealistic and not an innocuous approximation, in general [72] and in particular in the very delicate case of a biaxial nematic phase. It does not include or substantially alter the stability of the isotropic (I) phase, a very serious contender for any liquid-crystalline phase. When applied to mixtures, it can substantially underestimate the demixing gap [73]. In general, to assume that a dense system of particles well aligned yet freely rotating can be assimilated to a dense system of particles perfectly aligned is misguided. (In addition, any theory based on the Zwanzig model is not very prone to be readily falsifiable or verifiable by corresponding numerical experiments).

III. NUMERICAL SIMULATION METHOD AND CALCULATED QUANTITIES

Being short of a theory really capable of reliably tracing the complete phase diagram, i.e., a theory not only able to deal with fluid, isotropic and liquid-crystalline, phases but especially also allowing for the formation of a crystal phase (with a single exception [13], theoretical calculations had not attempted its inclusion) or a glassy state, of systems of such model particles, one has to resort to numerical simulation.

Systems of $N \in [576, 2400]$ hard spherocylinder dimers (Fig. 1) were considered for several values of $s^* = s/D \in [0, 6]$ and investigated with the Monte Carlo (MC) numerical simulation method [75,76] in the isobaric(-isothermal) (NPT) ensemble [77] using shape-and-size variable orthorhombic or triclinic computational boxes [78] and periodic boundary conditions. For each value of s^* considered, the MC-NPT runs were conducted at many values of pressure P, usually varied in a step of $0.1\frac{PD^3}{k_BT}$, with k_B the Boltzmann constant. These MC-NPT runs were organized in cycles, each of these cycles being on average constituted by N attempts to displace the centroid of a randomly selected particle; N attempts to rigidly and sequentially rotate a randomly selected particle around two randomly selected but noncoincident axes of the laboratory reference frame; one attempt to overturn a randomly selected particle; and one attempt to vary the computational box shape and size by varying a randomly selected element of the diagonal (if the computational box is constrained to be orthorhombic) or (upper) triangular (if the computational box is allowed to be triclinic) matrix $\mathbf{H}$ that relates real coordinates, $\mathbf{r}_\circ$, to suitably reduced coordinates, $\mathbf{q}_\circ$, of the particle centroids: $\mathbf{r}_\circ = \mathbf{H}\mathbf{q}_\circ$. For each of the attempted moves, the maximal size was fixed by requiring that the respective acceptance percentage was 20%–30% and never altered during a MC-NPT run, the overlap criterion between two hard spherocylinders dimers simply following from that, very simple [56], between two hard spherocylinder monomers. For each value of s^* and P considered, a first MC-NPT run started from either a simple orthorhombic crystalline configuration or a configuration obtained in a numerical simulation carried out at a nearby value of P and could last up to 10×10^6 MC cycles. From the last configuration generated in this MC-NPT run, a second MC-NPT run started and usually lasted at least 10^6 MC cycles, during which configurations were regularly saved and stored for the subsequent analysis.

This analysis consisted in the calculation of (1) the mean number density ϱ, hence the volume fraction $\phi = \varrho v$, with $v = (17/6)\pi D^3$ the particle volume, so as to determine the system equation of state; (2) several order parameters and (3) several real-space correlation functions as well as (4) the reciprocal-space structure factor, so as to identify the phases that a system forms and characterize their (micro)structure; and (5) the mean square displacement, so as to still have an indication of whether a phase can be qualified as fluid or solid while remaining well aware that the MC method should be distrusted anytime it is improperly employed to address dynamic properties.

The set of order parameters includes the following:

(1) The uniaxial nematic order parameter S_2. It was calculated following the usual procedure [79] that consists in (a) for each configuration, calculating the matrix $\mathbf{Q}^{\hat{\mathbf{u}}\hat{\mathbf{u}}}$ whose element $Q^{uu}_{\alpha,\beta}$ is defined as

$$Q^{uu}_{\alpha,\beta} = \frac{1}{N}\sum_{i=1}^{N}\frac{3}{2}u_{i\alpha}u_{i\beta} - \frac{1}{2}\delta_{\alpha,\beta} \tag{1}$$

with $\alpha, \beta = X, Y, Z$, the three axes of the laboratory reference frame, $u_{i\alpha}$ the α component of the unit vector $\hat{\mathbf{u}}$ of particle i, and $\delta_{\alpha,\beta}$ the Krönecker symbol; diagonalizing $\mathbf{Q}^{\hat{\mathbf{u}}\hat{\mathbf{u}}}$ to obtain the three eigenvalues and the respective eigenvectors; and taking the largest eigenvalue as the configuration uniaxial nematic order parameter and the associated eigenvector as the configuration $\hat{n}$; (b) taking the arithmetic mean of the configuration uniaxial nematic order parameter over the configurations, which finally constitutes the system uniaxial nematic order parameter S_2.

(2) The biaxial nematic order parameters, $S_{w_\perp}$ and $P_{C_{2h}}$. To detect whether a biaxial nematic ordering is present, quantify its extent, and further distinguish its nature, two order parameters were calculated.

The first, denoted $S_{w_\perp}$, served to detect and quantify the extent of the ordinary, D_{2h}-symmetric, biaxial nematic ordering. It is obtained by (a) for each configuration, calculating the (effectively 2×2) matrix $\mathbf{Q}^{\hat{\mathbf{w}}_\perp\hat{\mathbf{w}}_\perp}$ whose element $Q^{w_\perp w_\perp}_{\alpha,\beta}$ is defined as

$$Q^{w_\perp w_\perp}_{\alpha,\beta} = \frac{1}{N}\sum_{i=1}^{N} 2w_{\perp i\alpha}w_{\perp i\beta} - \delta_{\alpha,\beta} \tag{2}$$

with $w_{\perp i\alpha}$ the α component of the unit vector $\hat{\mathbf{w}}_\perp$ of the particle i, being $\hat{\mathbf{w}}_\perp = (\hat{\mathbf{w}} \times \hat{n})/|\hat{\mathbf{w}} \times \hat{n}|$; diagonalizing $\mathbf{Q}^{\hat{\mathbf{w}}_\perp\hat{\mathbf{w}}_\perp}$ to obtain the two eigenvalues and the respective eigenvectors; and taking the largest eigenvalue as the configuration biaxial nematic order parameter and the associated eigenvector as the configuration $\hat{m}$; (b) taking the arithmetic mean of the configuration biaxial nematic order parameter over the configurations, which finally constitutes the system biaxial nematic order parameter $S_{w_\perp}$.

The second, denoted $P_{C_{2h}}$, further distinguishes whether the biaxial nematic ordering detected and quantified via $S_{w_\perp}$ could actually be of C_{2h} symmetry, a check admittedly demanded just by the symmetry of the present hard particles rather than by a hope of indeed observing a C_{2h}-symmetric biaxial nematic phase. This biaxial nematic order parameter is defined as

$$P_{C_{2h}} = \left\langle \frac{1}{N} \left| \sum_{i=1}^{N} (\hat{\mathbf{u}}_i \cdot \hat{n})(\hat{\mathbf{w}}_{\perp i} \cdot \hat{m}) \right| \right\rangle \tag{3}$$

with $\langle\rangle$ indicating an arithmetic mean over configurations. It is equal to 0 even in the presence of a perfect D_{2h}-symmetric biaxial nematic ordering but equal to 1 in the presence of a perfect C_{2h}-symmetric biaxial nematic ordering.

(3) The smectic-*A* order parameter τ_A. It was calculated following the usual procedure that consists in (a) for each configuration, calculating the quantity

$$\max_{\ell} \frac{1}{N} \left| \sum_{j=1}^{N} e^{\mathrm{i}\mathbf{r}_{\circ j} \cdot \frac{2\pi}{\ell} \hat{n}} \right|, \tag{4}$$

which is taken as the configuration smectic-*A* order parameter while the value of ℓ at which this maximum occurs is taken as the configuration smectic-*A* spacing; (b) taking the arithmetic mean of the configuration smectic-*A* order parameter over the configurations, which finally constitutes the system smectic-*A* order parameter τ_A.

(4) The smectic-*C* order parameter τ_C. The usual procedure to calculate τ_A exploits the fact that one of the defining attributes of a smectic-*A* phase is its having the layer normal coincident with $\hat{n}$. One can realize that scanning the values of ℓ in search of the maximum of Eq. (4) is essentially nothing more than searching for the maximum of the structure factor $\mathcal{S}(\mathbf{k})$ (vide infra) among the reciprocal-lattice vectors of the form $\mathbf{k} = \frac{2\pi}{\ell}\hat{n}$. For a smectic-*C* phase, the direction of the layer normal is not *a priori* known. For each configuration, one can retrieve it by determining, among the reciprocal-lattice vectors compatible with the computational box, the one, $\mathbf{k}_{\max}$, at which $\mathcal{S}(\mathbf{k})$ shows the (most) prominent (Bragg) peak. This $\mathbf{k}_{\max}$ identifies the direction of the layer normal; $\theta_{\mathrm{tilt}} = \arccos{[(\mathbf{k}_{\max} \cdot \hat{n})/|\mathbf{k}_{\max}|]}$ is the tilt angle. The smectic-*C* order parameter can then be obtained by (a) for each configuration, calculating the quantity

$$\frac{1}{N} \left| \sum_{j=1}^{N} e^{\mathrm{i}\mathbf{r}_{\circ j} \cdot \mathbf{k}_{\max}} \right| \tag{5}$$

and (b) taking its arithmetic mean over the configurations. Since a smectic-*A* phase is a special smectic-*C* phase with a vanishing θ_{tilt}, the procedure can equally be applied to a smectic-*A* phase, thus consistently retrieving the smectic-*A* order parameter previously obtained via the usual procedure.

(5) The monomer hexatic order parameter $\psi_{6\mathrm{mono}}$. One can naturally view any configuration (packing) of hard spherocylinder dimers such as the one in Fig. 1 as a realization of a configuration (packing) of hard spherocylinder monomers. By adopting this view, the monomer hexatic order parameter adopts the definition of the usual hexatic order parameter [80]:

$$\psi_{6\mathrm{mono}} = \left\langle \frac{1}{N} \sum_{i=1}^{N} \left| \frac{1}{n_{\mathrm{vic}\,i}} \sum_{j=1}^{n_{\mathrm{vic}\,i}} e^{\mathrm{i}6\vartheta_{ij}} \right| \right\rangle, \tag{6}$$

which requires, for each configuration, to determine, for each hard spherocylinder monomer i, the number of its nearest neighbors $n_{\mathrm{vic}\,i}$, i.e., any hard spherocylinder j whose centroid lie at a distance $r_{\perp ij} = |\mathbf{r}_{\perp ij}| = |(\mathbf{r}_{\circ j} - \mathbf{r}_{\circ i}) \times \hat{n}| \leqslant r_{g_{\min}}$ from the centroid of i, $r_{g_{\min}}$ being the value of distance at which the $g(r)$ (vide infra) has its first minimum, and at a distance $r_{\parallel ij} = |(\mathbf{r}_{\circ j} - \mathbf{r}_{\circ i}) \cdot \hat{n}| \leqslant L$, and calculate the angle ϑ_{ij} that $\hat{\mathbf{r}}_{\perp ij}$, the direction of the fictitious "bond" between i and j, forms with an arbitrary axis $\hat{\mathbf{h}}$ such that $\hat{\mathbf{h}} \perp \hat{n}$. One natural by-product of these calculations is the distribution of n_{vic}, $p(n_{\mathrm{vic}})$.

The set of real-space pair correlation functions includes the following:

(1) $g(r)$. This is the most basic positional pair correlation function, proportional to the conditional probability density of finding the centroid of a particle j at a distance r from the centroid of a particle i. It can be defined as

$$g(r) = \frac{1}{N} \left\langle \frac{1}{\varrho} \sum_{i=1}^{N} \sum_{i \neq j}^{N} \delta(r - r_{ij}) \right\rangle \tag{7}$$

with $r_{ij} = |\mathbf{r}_{ij}| = |\mathbf{r}_{\circ j} - \mathbf{r}_{\circ i}|$ and $\delta()$ the δ function.

(2) $g_{\parallel}(r_{\parallel})$. This is the positional pair correlation function providing information on the correlation between two particle centroids along $\hat{n}$. It can be defined as

$$g_{\parallel}(r_{\parallel}) = \frac{1}{N} \left\langle \frac{1}{\varrho} \sum_{i=1}^{N} \sum_{i \neq j}^{N} \delta(r_{\parallel} - \mathbf{r}_{ij} \cdot \hat{n}) \right\rangle. \tag{8}$$

(3) $g_{\perp}(r_{\perp})$. This is the positional pair correlation function providing information on the correlation between two-particle centroids transverse to $\hat{n}$. It can be defined as

$$g_{\perp}(r_{\perp}) = \frac{1}{N} \left\langle \frac{1}{\varrho} \sum_{i=1}^{N} \sum_{i \neq j}^{N} \delta(r_{\perp} - |\mathbf{r}_{ij} \times \hat{n}|) \right\rangle. \tag{9}$$

(4) $\mathcal{G}_2^{\hat{\mathbf{u}}\hat{\mathbf{u}}}(r)$. This is a second-order orientational pair correlation function defined as

$$\mathcal{G}_2^{\hat{\mathbf{u}}\hat{\mathbf{u}}}(r) = \left\langle \frac{\sum_{i=1}^{N} \sum_{i \neq j}^{N} P_2(\hat{\mathbf{u}}_i \cdot \hat{\mathbf{u}}_j)\delta(r - r_{ij})}{\sum_{i=1}^{N} \sum_{i \neq j}^{N} \delta(r - r_{ij})} \right\rangle \tag{10}$$

with $P_2()$ the second-order Legendre polynomial. This function measures the degree of correlation in the orientations of the axes $\hat{\mathbf{u}}$ of two particles whose centroids are separated by a distance r.

(5) $\mathcal{G}_2^{\hat{\mathbf{u}}\hat{\mathbf{r}}}(r)$. This is a second-order bond-orientational pair correlation function defined as

$$\mathcal{G}_2^{\hat{\mathbf{u}}\hat{\mathbf{r}}}(r) = \left\langle \frac{\sum_{i=1}^{N} \sum_{i \neq j}^{N} P_2(\hat{\mathbf{u}}_i \cdot \hat{\mathbf{r}}_{ij})\delta(r - r_{ij})}{\sum_{i=1}^{N} \sum_{i \neq j}^{N} \delta(r - r_{ij})} \right\rangle \tag{11}$$

with $\hat{\mathbf{r}}_{ij} = \mathbf{r}_{ij}/r_{ij}$. This function measures the degree of orientational ordering of the fictitious "bond" $\mathbf{r}_{ij}$, established between the centroids of two particles i and j, separated by a distance r, with respect to $\hat{\mathbf{u}}_i$.

(6) $\mathcal{G}_2^{\hat{\mathbf{w}}_{\perp}\hat{\mathbf{w}}_{\perp}}(r)$. This is a second-order orientational pair correlation function measuring the degree of correlation in the orientations of the axes $\hat{\mathbf{w}}_{\perp}$ of two particles whose centroids are separated by a distance r. It is defined as

$$\mathcal{G}^{\hat{\mathbf{w}}_{\perp}\hat{\mathbf{w}}_{\perp}}(r) = \left\langle \frac{\sum_{i=1}^{N} \sum_{i \neq j}^{N} [2(\hat{\mathbf{w}}_{\perp i} \cdot \hat{\mathbf{w}}_{\perp j})^2 - 1]\delta(r - r_{ij})}{\sum_{i=1}^{N} \sum_{i \neq j}^{N} \delta(r - r_{ij})} \right\rangle. \tag{12}$$

(7) $\mathcal{G}^{\hat{\mathbf{u}}\hat{\mathbf{w}}_\perp}(r)$. This is a special orientational pair correlation function providing information on the presence of a C_{2h}-symmetric biaxial nematic ordering in the system. It is defined as

$$\mathcal{G}^{\hat{\mathbf{u}}\hat{\mathbf{w}}_\perp}(r) = \left\langle \frac{\sum_{i=1}^{N}\sum_{i\neq j}^{N}(\hat{\mathbf{u}}_i\cdot\hat{\mathbf{u}}_j)(\hat{\mathbf{w}}_{\perp i}\cdot\hat{\mathbf{w}}_{\perp j})\delta(r-r_{ij})}{\sum_{i=1}^{N}\sum_{i\neq j}^{N}\delta(r-r_{ij})} \right\rangle. \tag{13}$$

In addition to the real-space pair correlation functions, the reciprocal-space structure factor $\mathcal{S}(\mathbf{k})$ was also calculated. More precisely, it is its orientational average $\mathcal{S}(k)$ that was calculated as

$$\mathcal{S}(k) = \left\langle \frac{1}{N}\left|\sum_{j=1}^{N} e^{i\mathbf{k}\cdot\mathbf{r}_{\circ j}}\right|^2 \right\rangle_{\hat{\mathbf{k}}} \tag{14}$$

with $\mathbf{k}$ a reciprocal-lattice vector compatible with the computational box, $k = |\mathbf{k}|$ and $\langle\rangle_{\hat{\mathbf{k}}}$ signifying a suitable orientational average over the reciprocal lattice vectors sharing the same modulus in addition to an arithmetic mean over configurations.

IV. RESULTS

For each value of $s^* \in [0, 6]$ considered, the sequence of phases that a system of corresponding hard spherocylinder dimers form was determined following the protocol of Sec. III. These individual phase diagrams are separately depicted and fully described in the Supplemental Material [45]. By critically collecting all the relevant data acquired on the several systems of hard spherocylinder dimers that were investigated, a complete phase diagram can then be sketched in the plane s^* versus ϕ (Fig. 2).

The liquid-crystalline phases are naturally bracketed by the omnipresent isotropic fluid, at low ϕ, and solid, at high ϕ, phases.

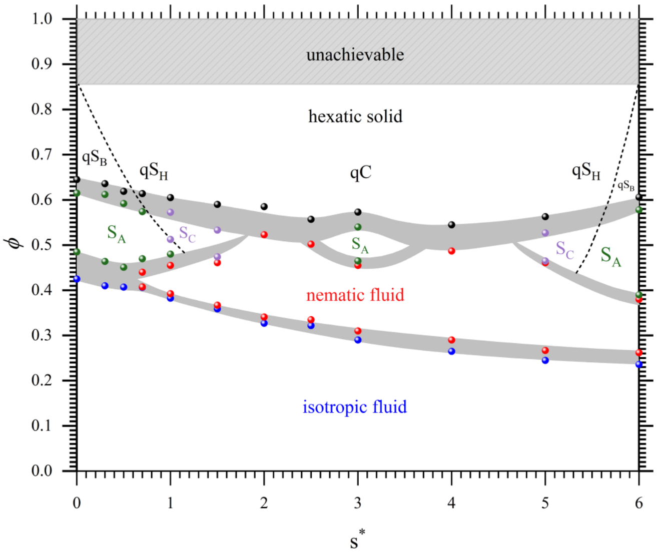

FIG. 2. Sketch of the phase diagram of systems of the hard C_{2h}-symmetric particles of Fig. 1 in the plane shift $s^* = s/D$ versus volume fraction ϕ. The several phases are indicated by the corresponding label or name. The dashed lines separate smectic-A phase or quasismectic B phase from smectic-C phase or quasismectic H phase. The points correspond to phase coexistence data obtained as discussed in the Supplemental Material [45]. The gray zones, whose delimiting curves smoothly fit the respective points, correspond to phase coexistence. The hatched zone is for values of ϕ that are, essentially, unachieveable, being the ordinate value of the lower horizontal line equal to 0.856…, the lower bound for the volume fraction of the densest-known packings common to any abscissa value.

In the present context, the solid phase is generally characterized by a monomeric hexagonal order. Depending on the value of s^*, the hexatic (Hex) solid phase can further take up the form of a: quasismectic B (qS_B) at $s^* \to 0$ or $s^* \to 6$; quasismectic H (qS_H) at values of s^* slightly larger than 0 or slightly smaller than 6; quasicolumnar (qC) at intermediate values of s^*; the prefix "quasi" having been added to just indicate that those forms are rather more referrable to the constituent hard spherocylinder monomers than to the actual hard spherocylinder dimers. Dense packings of hard spherocylinder dimers, the detailed and specific investigation of those, among them, that reach the maximal (optimal) value of ϕ being not part of the present study, can generally be constructed with a value of ϕ at least as high as $17\sqrt{3}\pi/108 = 0.856\ldots$ and occasionally as high as $(17\pi/6)/(\sqrt{2}+5\sqrt{3}) = 0.883\ldots$ but the upmost limit value of $\phi = 1$ cannot be reached because hard spherocylinders are not space fillers. The former value of 0.856… corresponds to the value of ϕ reached by packings of hard spherocylinders with $L/D = 5$ disposed in a hexagonal (the hexagonal lattice being the densest packing of two-dimensional hard disks [83]) columnar fashion, while the latter value of 0.883… corresponds to the value of ϕ reached by densest Bravais lattice packing of hard spherocylinders with $L/D = 5$, one of the infinitely many densest-known (very much probably, *sic et simpliciter*, densest [81,82]) stacking-variant packings of hard spherocylinders with such a value of L/D. While the former lower value of ϕ is common to any value of s^*, the latter higher value of ϕ is specific to $s = 0$ because only packings of these actual hard spherocylinder dimers reach the same value of ϕ that the Bravais lattice packing of the constituent hard spherocylinder monomers does. Then, one can take the value of $\phi = 0.856\ldots$ as a lower bound for the maximal (optimal) value of ϕ for any s^*. This is expected and nothing more than what is already known for hard spherocylinders, a packing of such hard spherocylinder dimers *a fortiori* being a packing of hard spherocylinder monomers. Besides affecting the maximal (optimal) value of ϕ as a function of s^*, the dimeric nature of the present hard particles especially emerges from its being responsible for the introduction of a special type of bond-orientational ordering in terms of the unit vectors $\hat{\mathbf{w}}$. If viewed from a direction parallel to $\hat{n}$, such very dense packings of hard spherocylinders dimers, irrespective of whether their structure being further classified as quasismectic B, quasismectic H, or quasicolumnar, resemble a system of hard two-dimensional disk dimers. For a system of hard two-dimensional disk dimers, it has been shown that the high-density stable phase is a nonperiodic solid [84]. This conclusion carries over to systems of hard spherocylinders dimers, as Fig. 4 of the Supplemental Material [45] illustrates.

Smectic phase regions exist at the two extremes of the s^* interval, while a peculiar smectic-*A* phase "pocket" also shows up around $s^* = 3$. Within the two extremal smectic phase regions, the (uniaxial) *A* (S_{Au}) phase that forms at $s^* = 0$ and $s^* = 6$ gives gradually way to the (inherently biaxial) *C* (S_C) phase as s^* respectively increases or decreases from the corresponding extremal value of 0 or 6. The smectic-*A* phase at $s^* = 3$ as well as the smectic-*A* phase at $s^* \to 6$ are characterized by a layer spacing coincident with the overall shift and therefore shorter than the overall length of a hard spherocylinder dimer. Thus, while at $s^* \to 6$ the layer-spacing length ordinarily approximately coincides with that of the hard spherocylinder monomer, at $s^* = 3$ it is approximately equal to $3D$, that is, in this case, the length of the layer spacing is peculiarly short: such a short-layer-spacing smectic-*A* phase is unrealizable in a system of hard spherocylinders with $L/D = 2$ as such a system transits from the isotropic phase directly to a crystal phase [58]. The three smectic phase regions of existence are disjoint, and each extremal region is separated from the middle "pocket" by a region where the uniaxial nematic phase extends up to relatively large values of ϕ where the hexatic solid phase becomes stable.

The complete phase diagram of Fig. 2 is rather symmetric with respect to $s^* = 3$. Its symmetry is imperfect for chiefly two reasons. First, in the neighborhood of $s^* = 0$, no nematic phase forms but the isotropic fluid transits directly to the smectic-*A* fluid. By gluing together two hard spherocylinders that, as monomers, do form the uniaxial version of such a liquid-crystalline phase [58], thus constructing hard biaxial particles that much resemble those hard boardlike particles long hypothesized to give rise to the biaxial version of such a liquid-crystalline phase, no nematic phase of any sort rather ironically forms. In the neighborhood of $s^* = 6$, the uniaxial nematic phase is instead stable in an ample interval of ϕ. Second, the values of ϕ at the isotropic-nematic phase coexistence, incipient at $s^* \simeq 1$, gently decline with increasing s^*: an expected effect of the increasing overall "length" -to- "width" ratio of these hard particles.

Out of curiosity, one may imagine how the phase diagram of Fig. 2 would get modified were hard spherocylinder dimers as in Fig. 1 with $L/D \neq 5$ to be considered. For values of L/D smaller than 5 not more than a couple of units, the relevance that the present hard spherocylinder dimer model has to thermotropic low-molecular-mass LCs would be preserved, but those hard spherocylinder dimers would have a progressively diminishing tendency to form any nematic phase. Naturally, the latter tendency would progressively increase as L/D gets larger than 5. For $s^* \to 0$ too, a nematic phase would finally turn up, while, for larger value of s^*, the isotropic-nematic coexistence would shift to lower ϕ. The combined action of these two changes, together with the probable nearly constancy of the values of ϕ at which the hexatic solid phase becomes stable, would broaden and deepen the region of existence of the nematic phase. However, larger values of L/D would increasingly be detrimental to the relevance that the present hard spherocylinder model has to thermotropic low-molecular-mass LCs, without ensuring an increased hope of observing, at the highest density within the nematic phase, the surge of a biaxial orientational ordering. In this respect, more auspicable should be keeping the same value of $L/D = 5$, fixing s^* at $\simeq 2$ or $\simeq 4$ and considering hard spherocylinder trimers as obtained by gluing to either hard spherocylinder dimer one more aligned hard spherocylinder monomer with the same value of shift.

V. CONCLUSIONS

Two, rather intertwined, are the principal results of the present study. One result is the absence of a biaxial nematic phase: when letting the system form (partially) positionally ordered phases, these manifest and prevail. The other result is the observation that, for values of $s \simeq 2D$ and $s \simeq 4D$, no liquid-crystalline phase is stable other than the nematic phase.

Even though no sign of biaxial orientational ordering has been detected within this nematic phase, to have observed how smectic phases could be destabilized in a model but, if viewed not only from the lyotropic colloidal LC side but also from the thermotropic low-molecular-mass LC side, realistic pure system constitutes a stone on which subsequent, both theoretical and experimental, research activities may make their first step.

Theoretically, one could investigate the phase behavior of hard spherocylinder trimers with those "optimal" values of shift $s \simeq 2D$ or $s \simeq 4D$ and probe whether they are more inclined to form a biaxial nematic phase; in general, it should be interesting to consider, in lieu of hard cuboidal particles, hard (sphero)parallelogrammic prismlike particles, in particular with a shape similar to the present "optimal" hard spherocylinder dimers or to those hard spherocylinder trimers.

Experimentally, the synthesis and characterization, including the phase behavior, of low-molecular-mass molecules with a shape resembling that of the present "optimal" hard spherocylinder dimers or that of those hard spherocylinder trimers may be an effort worth its while.

ACKNOWLEDGMENTS

C.D'U. and G. Celebre acknowledge the support of the University of Calabria, while G. Cinacchi acknowledges the support of the Government of Spain under Grants No. FIS2013-47350-C5-1-R, No. MDM-2014-0377, and No. FIS2017-86007-C3-1-P.

---

[1] P. M. Chaikin and T. C. Lubensky, *Principles of Condensed Matter Physics* (Cambridge University Press, Cambridge, 1995).

[2] L. M. Blinov, *Structure and Properties of Liquid Crystals* (Springer, Dordrecht, 2011).

[3] M. J. Freiser, Phys. Rev. Lett. **24**, 1041 (1970); Mol. Cryst. Liq. Cryst. **14**, 165 (1971).

[4] C. S. Shih and R. Alben, J. Chem. Phys. **57**, 3055 (1972); R. Alben, Phys. Rev. Lett. **30**, 778 (1973).

[5] J. P. Straley, Phys. Rev. A **10**, 1881 (1974).

[6] N. Boccara, R. Mejdani, and L. de Seze, J. Physique **38**, 149 (1977).

[7] L. J. Yu and A. Saupe, Phys. Rev. Lett. **45**, 1000 (1980).

[8] F. Hessel and H. Finkelmann, Polym. Bull. **15**, 349 (1986); F. Hessel, R. P. Herr, and H. Finkelmann, Makromol. Chem. **188**, 1597 (1987); F. Brömmel, W. Stille, H. Finkelmann, and A. Hoffmann, Soft Matter **7**, 2387 (2011).

[9] A. M. Somoza and P. Tarazona, Phys. Rev. Lett. **61**, 2566 (1988); J. Chem. Phys. **91**, 517 (1989).

[10] B. M. Mulder, Phys. Rev. A **39**, 360 (1989); Liq. Cryst. **8**, 527 (1990).

[11] R. Holyst and A. Poniewierski, Mol. Phys. **69**, 193 (1990).

[12] M. P. Allen, Liq. Cryst. **8**, 499 (1990); P. J. Camp and M. P. Allen, J. Chem. Phys. **106**, 6681 (1997).

[13] M. P. Taylor and J. Herzfeld, Phys. Rev. A **44**, 3742 (1991).

[14] F. Biscarini, C. Chiccoli, P. Pasini, F. Semeria, and C. Zannoni, Phys. Rev. Lett. **75**, 1803 (1995); C. Chiccoli, P. Pasini, F. Semeria, and C. Zannoni, Int. J. Mod. Phys. C **10**, 469 (1999); G. S. Preeti, K. P. N. Murthy, V. S. S. Sastry, C. Chiccoli, P. Pasini, R. Berardi, and C. Zannoni, Soft Matter **7**, 11483 (2011).

[15] S. Sarman, J. Chem. Phys. **104**, 342 (1996); **107**, 3144 (1997); Int. J. Thermophys. **19**, 1073 (1998); Phys. Chem. Chem. Phys. **2**, 3831 (2000).

[16] P. I. C. Teixera, A. J. Masters, and B. M. Mulder, Mol. Cryst. Liq. Cryst. **323**, 167 (1998).

[17] R. Berardi and C. Zannoni, J. Chem. Phys. **113**, 5971 (2000); Mol. Cryst. Liq. Cryst. **396**, 177 (2003); R. Berardi, L. Muccioli, and C. Zannoni, J. Chem. Phys. **128**, 024905 (2008).

[18] K. Praefcke, Mol. Cryst. Liq. Cryst. **364**, 15 (2001); Braz. J. Phys. **32**, 564 (2002).

[19] G. R. Luckhurst, Thin Solid Films **393**, 40 (2001).

[20] A. G. Vanakaras, M. A. Bates, and D. J. Photinos, Phys. Chem. Chem. Phys. **5**, 3700 (2003).

[21] D. W. Bruce, Chem. Rec. **4**, 10 (2004).

[22] K. Severing and K. Saalwächter, Phys. Rev. Lett. **92**, 125501 (2004); K. Severing, E. Stibal-Fischer, A. Hasenhindl, H. Finkelmann, and K. Saalwächter, J. Phys. Chem. B **110**, 15680 (2006).

[23] B. R. Acharya, A. Primak, T. J. Dingemans, E. T. Samulski, and S. Kumar, Pramana **61**, 231 (2003); L. A. Madsen, T. J. Dingemans, M. Nakata, and E. T. Samulski, Phys. Rev. Lett. **92**, 145505 (2004); B. R. Acharya, A. Primak, and S. Kumar, *ibid.* **92**, 145506 (2004).

[24] G. R. Luckhurst, Nature (London) **430**, 413 (2004); Angew. Chem. Int. Ed. **44**, 2834 (2005); (a simple comment might be pertinent: the reader may feel a change of tone, from rather decided to quite doubtful, between the former and the latter of these two commentaries, notwithstanding their being separated by an interval of only one year).

[25] K. Merkel, A. Kocot, J. K. Vij, R. Korlacki, G. H. Mehl, and T. Meyer, Phys. Rev. Lett. **93**, 237801 (2004); J. L. Figueirinhas, C. Cruz, D. Filip, G. Feio, A. C. Ribeiro, Y. Frère, T. Meyer, and G. H. Mehl, *ibid.* **94**, 107802 (2005); K. Neupane *et al.*, *ibid.* **97**, 207802 (2006).

[26] G. Cordoyiannis, D. Apreutesei, G. H. Mehl, C. Glorieux, and J. Thoen, Phys. Rev. E **78**, 011708 (2008); C. Cruz, J. L. Figueirinhas, D. Filip, G. Feio, A. C. Ribeiro, Y. Frère, T. Meyer, and G. H. Mehl, *ibid.* **78**, 051702 (2008); D. Filip, C. Cruz, P. J. Sebastião, M. Cardoso, A. C. Ribeiro, M. Vilfan, T. Meyer, P. H. J. Kouwer, and G. H. Mehl, *ibid.* **81**, 011702 (2010); K. Merkel, M. Nagaraj, A. Kocot, A. Kohlmeier, G. H. Mehl, and J. K. Vij, J. Chem. Phys. **136**, 094513 (2012); S. Polineni, J. L. Figueirinhas, C. Cruz, D. A. Wilson, and G. H. Mehl, *ibid.* **138**, 124904 (2013).

[27] A. G. Vanakaras and D. J. Photinos, J. Chem. Phys. **128**, 154512 (2008).

[28] R. Berardi, L. Muccioli, S. Orlandi, M. Ricci, and C. Zannoni, J. Phys. Condens. Matt. **20**, 463101 (2008).

[29] P. K. Karahaliou, A. G. Vanakaras, and D. J. Photinos, J. Chem. Phys. **131**, 124516 (2009).

[30] E. van den Pol, A. V. Petukhov, D. M. E. Thies-Weesie, D. V. Byelov, and G. J. Vroege, Phys. Rev. Lett. **103**, 258301 (2009).

[31] C. Tschierske and D. J. Photinos, J. Mater. Chem. **20**, 4263 (2010).

[32] E. T. Samulski, Liq. Cryst. **37**, 669 (2010); O. Francescangeli and E. T. Samulski, Soft Matter **6**, 2413 (2010); O. Francescangeli, F. Vita, C. Ferrero, T. Dingemans, and E. T. Samulski, *ibid.* **7**, 895 (2011).

[33] S. Belli, A. Patti, M. Dijkstra, and R. van Roij, Phys. Rev. Lett. **107**, 148303 (2011); S. Belli, M. Dijkstra, and R. van Roij, J. Phys. Condens. Matt. **24**, 284128 (2012).

[34] M. Lehmann, Liq. Cryst. **38**, 1389 (2011).

[35] S. D. Peroukidis and A. G. Vanakaras, Soft Matter **9**, 7419 (2013).

[36] Y. K. Kim, B. Senyuk, S. T. Shin, A. Kohlmeier, G. H. Mehl, and O. D. Lavrentovich, Soft Matter **10**, 500 (2014).

[37] G. Celebre, J. Mol. Liq. **209**, 104 (2015); G. Celebre, C. D'Urso, and M. Porto, *ibid.* **248**, 847 (2017).

[38] G. R. Luckhurst and T. J. Sluckin, editors, *Biaxial Nematic Liquid Crystals: Theory, Simulation and Experiment* (John Wiley & Sons, Chichester, 2015).

[39] Y. K. Kim, G. Cukrov, F. Vita, E. Scharrer, E. T. Samulski, O. Francescangeli, and O. D. Lavrentovich, Phys. Rev. E **93**, 062701 (2016).

[40] A. Cuetos, M. Dennison, A. Masters, and A. Patti, Soft Matter **13**, 4720 (2017).

[41] S. Dussi, N. Tasios, T. Drwenski, R. van Roij, and M. Dijkstra, Phys. Rev. Lett. **120**, 177801 (2018).

[42] For example, by constraining the orientations of the particles along a few directions or omitting, in one or another way, dense(r) (partially) positionally ordered phases that would actually preempt the biaxial nematic phase in the equilibrium phase diagram.

[43] The thermotropic low-molecular-mass LCs are the class of LCs where a biaxial nematic phase has long been sought because its finding will presumably be technologically relevant.

[44] Concerning the past claims made in the last years of the 20th century, one may consult Refs. [18,19]. Concerning the recent claims made in the first years of the 21st century, cf. Ref. [23] with Ref. [39] and cf. Ref. [25] with Ref. [36]. Reference [39] definitely disclaims the claims initially made in Ref. [23] to have observed a biaxial nematic phase and subsequently made in Ref. [32] to have observed an external-field–induced biaxial cybotactic nematic [46] phase in a system of banana-shaped molecules. Reference [36] definitely disclaims the claims initially made in Ref. [25] and apparently confirmed in a number of subsequent works [26] to have observed a biaxial nematic phase in a system of tetrapodes.

[45] See Supplemental Material at http://link.aps.org/supplemental/10.1103/PhysRevE.100.012709 for the full description of the obtained results.

[46] A. De Vries, Mol. Cryst. Liq. Cryst. **10**, 219 (1970); L. V. Azároff, Proc. Natl. Acad. Sci. USA **77**, 1252 (1980).

[47] L. Onsager, Ann. N. Y. Acad. Sci. **51**, 627 (1949).

[48] G. R. Luckhurst, S. Naemura, T. J. Sluckin, T. B. T. To, and S. Turzi, Phys. Rev. E **84**, 011704 (2011); R. Hashim, G. R. Luckhurst, and H. S. Nguan, arXiv:1403.0798v1.

[49] N. Abbagnano, *Storia della Filosofia; Volume II: la filosofia medievale (la Patristica e la Scolastica)* (TEA, Milan, 1995).

[50] E. G. Hohenstein and C. D. Sherrill, WIREs Comput. Mol. Sci. **2**, 304 (2012).

[51] H. C. Longuet-Higgins and B. Widom, Mol. Phys. **8**, 549 (1964); B. Widom, Science **157**, 375 (1967).

[52] H. Reiss, Adv. Chem. Phys. **9**, 1 (1965).

[53] P. N. Pusey and W. van Megen, Nature (London) **320**, 340 (1986); H. Maeda and Y. Maeda, Phys. Rev. Lett. **90**, 018303 (2003).

[54] W. W. Wood, and R. R. Parker, J. Chem. Phys. **27**, 720 (1957); W. W. Wood and J. D. Jacobson, *ibid.* **27**, 1207 (1957); W. W. Wood, R. R. Parker, and J. D. Jacobson, Nuovo Cimento **9S1**, 133 (1958); B. J. Alder and T. E. Wainwright, J. Chem. Phys. **27**, 1208 (1957); T. E. Wainwright and B. J. Alder, Nuovo Cimento **9S1**, 116 (1958); W. G. Hoover and F. H. Ree, J. Chem. Phys. **49**, 3609 (1968); J. D. Bernal, Proc. Roy. Soc. London **280**, 299 (1964).

[55] A. Rahman, Phys. Rev. **136**, A405 (1964); L. Verlet, *ibid.* **159**, 98 (1967); **165**, 201 (1968); D. Levesque and L. Verlet, Phys. Rev. A **2**, 2514 (1970); J. P. Hansen and L. Verlet, Phys. Rev. **184**, 151 (1969); J. A. Barker and D. Henderson, J. Chem. Phys. **47**, 2856 (1967); **47**, 4714 (1967); D. Levesque and L. Verlet, Phys. Rev. **182**, 307 (1969); J. A. Barker and D. Henderson, Rev. Mod. Phys. **48**, 587 (1976); D. Chandler and J. D. Weeks, Phys. Rev. Lett. **25**, 149 (1970); J. D. Weeks, D. Chandler, and H. C. Andersen, J. Chem. Phys. **54**, 5237 (1971); L. Verlet and J. J. Weis Phys. Rev. A **5**, 939 (1972); H. C. Andersen, D. Chandler, and J. D. Weeks, Adv. Chem. Phys. **34**, 105 (1976); D. Chandler, J. D. Weeks, and H. C. Andersen, Science **220**, 787 (1983).

[56] The overlap criterion between two hard spherocylinders amounts to calculating the shortest distance between two three-dimensional segments.

[57] M. Hosino, H. Nakano, and H. Kimura, J. Phys. Soc. Jpn. **46**, 1709 (1979); **47**, 740 (1979).

[58] D. Frenkel, J. Phys. Chem. **91**, 4912 (1987); D. Frenkel, H. N. W. Lekkerkerker, and A. Stroobants, Nature (London) **332**, 822 (1988); P. Bolhuis and D. Frenkel, J. Chem. Phys. **106**, 666 (1997).

[59] J. Vieillard-Baron, J. Chem. Phys. **56**, 4729 (1972).

[60] J. W. Perram and M. S. Wertheim, J. Comput. Phys. **58**, 409 (1985).

[61] D. Frenkel, B. M. Mulder and J. P. McTague, Phys. Rev. Lett. **52**, 287 (1984); D. Frenkel and B. M. Mulder, Mol. Phys. **55**, 1171 (1985).

[62] M. P. Allen and C. P. Mason, Mol. Phys. **86**, 467 (1995); P. J. Camp, C. P. Mason, M. P. Allen, A. A. Khare, and D. A. Kofke, J. Chem. Phys. **105**, 2837 (1996).

[63] G. Odriozola, J. Chem. Phys. **136**, 134505 (2012); G. Bautista-Carvajal, A. Moncho-Jordá, and G. Odriozola, *ibid.* **138**, 064501 (2013).

[64] The case of rod-disk mixtures is rather emblematic. If mixing cylindrically symmetric rodlike and cylindrically symmetric disklike particles may superficially look as a straightforward way to obtain a N_{bo} phase [65], it proved not to be so as such mixtures strongly tend to separate in a rod-rich phase and a disk-rich phase [66], neither able to form a N_{bo} phase (unless that natural tendency is not deceptively impeded by unrealistically making only the rod-disk pair attractively interact and that with an extremely large attractive-well range [67]).

[65] R. Alben, J. Chem. Phys. **59**, 4299 (1973); Y. Rabin, W. E. McMullen, and W. M. Gelbart, Mol. Cryst. Liq. Cryst. **89**, 67 (1982); A. Stroobants and H. N. W. Lekkerkerker, J. Phys. Chem. **88**, 3669 (1984).

[66] P. Palffy-Muhoray, J. R. de Bruyn, and D. A. Dunmur, Mol. Cryst. Liq. Cryst. **127**, 301 (1985); J. Chem. Phys. **82**, 5294 (1985); S. R. Sharma, P. Palffy-Muhoray, B. Bergersen, and D. A. Dunmur, Phys. Rev. A **32**, 3752 (1985); P. J. Camp, M. P. Allen, P. G. Bolhuis, and D. Frenkel, J. Chem. Phys. **106**, 9270 (1997); F. M. van der Kooij and H. N. W. Lekkerkerker, Phys. Rev. Lett. **84**, 781 (2000).

[67] A. Cuetos, A. Galindo, and G. Jackson, Phys. Rev. Lett. **101**, 237802 (2008).

[68] Consider a system of hard biaxial particles with height H, breadth B, and depth W. The optimal value of B that would promote the formation of a biaxial nematic phase is $B = \sqrt{HW}$ [5]. In order to observe a nematic ordering along a transverse direction, one should assume a minimal value of $B/W \approx 3$. Thus, a minimal value of $H/W \approx 9$ results. The actual shape of the hard particles determines whether these minimal values are sufficient or larger values of B/W and then H/W are instead required, very similarly to what happens with systems of hard uniaxial particles and the uniaxial nematic phase, with a system of hard uniaxial ellipsoids (spheroids) with a length-to-width ratio less than 3 being able to exhibit a nematic phase [61–63] while hard spherocylinders with a length-to-width ratio more than 4 are needed for a system of them to exhibit a nematic phase [58]. These simple considerations apply to the results of Ref. [41].

[69] Grossly speaking, but perhaps not so much, the problem of finding a hard biaxial particle model with so a particular shape that, notwithstanding having a moderate size, can give rise to a thermodynamically stable biaxial nematic phase is, *mutatis mutandis*, equivalent to the problem of finding a hard elongate (flat) uniaxial particle model with such a particular shape that, notwithstanding its length-to-width (diameter-to-thickness) ratio is as small as ≈2, can give rise to a thermodynamically stable uniaxial nematic phase.

[70] Systems of hard [12] or soft [17] biaxial ellipsoidal particles were already shown to form a N_{bo} phase. However, differently from an ellipsoidal colloidal particle, it is admittedly arduous to realize an "ellipsoidal" molecule.

[71] R. W. Zwanzig, J. Chem. Phys. **39**, 1714 (1963).

[72] J. P. Straley, J. Chem. Phys. **57**, 3694 (1972).

[73] For example, cf. the phase diagrams of the binary mixtures of Ref. [20], obtained by considering hard cuboidal particles with

the same cross section but different height and constraining them to be perfectly parallel, showing no demixing regions, with the phase diagrams of the binary mixtures of Ref. [74], obtained by considering hard spherocylinders with the same diameter but different length and freely rotating, showing wide demixing regions.

[74] G. Cinacchi, L. Mederos, and E. Velasco, J. Chem. Phys. **121**, 3854 (2004).

[75] N. Metropolis, A. W. Rosenbluth, M. N. Rosenbluth, A. H. Teller, and E. Teller, J. Chem. Phys. **21**, 1087 (1953).

[76] M. P. Allen and D. J. Tildesley, *Computer Simulation of Liquids* (Clarendon Press, Oxford, 1987); W. Krauth, *Statistical Mechanics: Algorithms and Computations* (Oxford University Press, Oxford, 2006).

[77] W. W. Wood, J. Chem. Phys. **48**, 415 (1968); **52**, 729 (1970).

[78] R. Najafabadi and S. Yip, Scr. Metall. **17**, 1199 (1983); S. Yashonath and C. N. R. Rao, Mol. Phys. **54**, 245 (1985).

[79] J. Vieilliard-Baron, Mol. Phys. **28**, 809 (1974); R. D. Mountain and T. W. Rijgrok, Physica A **89**, 522 (1977).

[80] B. I. Halperin and D. R. Nelson, Phys. Rev. Lett. **41**, 121 (1978); D. R. Nelson and B. I. Halperin, Phys. Rev. B **19**, 2457 (1979).

[81] A. Bezdek and W. Kuperberg, Mathematika **37**, 74 (1990).

[82] S. Torquato and Y. Jiao, Phys. Rev. E **86**, 011102 (2012).

[83] L. Fejes-Tóth, Math. Z. **46**, 83 (1940); J. Conway and N. J. A. Sloane, *Sphere Packings, Lattices and Groups* (Springer-Verlag, New York, 1999).

[84] A. C. Brańka and K. W. Wojciechowski, Mol. Phys. **56**, 1419 (1985); K. W. Wojciechowski, Phys. Lett. A **122**, 377 (1987); K. W. Wojciechowski, D. Frenkel, and A. C. Brańka, Phys. Rev. Lett. **66**, 3168 (1991); K. W. Wojciechowski, A. C. Brańka, and D. Frenkel, Physica A **196**, 519 (1993).